Direct determination of the crystal field parameters of Dy, Er, and Yb impurities in the skutterudite compound $CeFe_4P_{12}$ by electron spin resonance

D. J. Garcia,[1,2] F. A. Garcia,[1] J. G. S. Duque,[1] P. G. Pagliuso,[1] C. Rettori,[1] P. Schlottmann,[3] M. S. Torikachvili,[4] and S. B. Oseroff[4]

[1]*Instituto de Física "Gleb Wataghin," UNICAMP, Campinas, SP 13083-970, Brazil*

[2]*Consejo Nacional de Investigaciones Científicas y Técnicas (CONICET) and Centro Atómico Bariloche, S.C. de Bariloche (CP8400), Río Negro, Argentina*

[3]*Department of Physics, Florida State University, Tallahassee, Florida 32306, USA*

[4]*San Diego State University, San Diego, California 92182-1233, USA*

(Received 16 June 2008; published 25 November 2008)

Despite extensive research on the skutterudites for the last decade, their electric crystalline field ground state is still a matter of controversy. We show that electron spin resonance (ESR) measurements can determine the full set of crystal field parameters (CFPs) for the T_h cubic symmetry ($Im3$) of the $Ce_{1-x}R_xFe_4P_{12}$ (R=Dy, Er, Yb; $x \lesssim 0.003$) skutterudite compounds. From the analysis of the ESR data the three CFPs B_4^c, B_6^c, and B_6^t were determined for each of these rare earths at the Ce^{3+} site. The field and temperature dependence of the measured magnetization for the doped crystals is in excellent agreement with the one predicted by the CFPs B_n^m derived from ESR.

DOI: 10.1103/PhysRevB.78.174428 PACS number(s): 75.10.Dg, 71.70.Ch, 76.30.Kg

I. INTRODUCTION

The filled skutterudite compounds RT_4X_{12}, where R is a rare earth or actinide, T is a transition metal (Fe, Ru, and Os), and X is a pnictogen (P, As, and Sb), crystallize in the $LaFe_4P_{12}$ structure with space group $Im3$ and local point symmetry T_h for the R ions. Also recently a new skutterudite family, $(Sr,Ba)Pt_4Ge_{12}$, was found.[1] The R ion is surrounded by 8 transition-metal ions forming a cube, and 12 pnictogen ions that form a slightly deformed icosahedron.[2] These materials exhibit a broad range of strongly correlated electron phenomena.[3–5] In addition, the antimonite members are potential thermoelectric materials due to their enhanced Seebeck coefficient.[6,7]

It has been assumed for a long time that the description of the electric crystalline field (CF) of the cubic point groups T, T_h, O, T_d, and O_h is the same for all of them. Recently, Takegahara *et al.*[8] studied the CF for cubic point groups using group theory and a simple point-charge model and found that the above was not correct. Takegahara *et al.*[8] noticed that due to the absence of two symmetry operations in the T and T_h groups, namely, the C_4 and C_2' rotations,[9] the CF Hamiltonian (H_{CF}) allows for additional sixth-order terms with an extra crystal field parameter (CFP), B_6^t. Therefore, for T_h symmetry, in terms of Steven's operators[10] H_{CF} should be written as

$$H_{CF} = B_4^c(O_4^0 + 5O_4^4) + B_6^c(O_6^0 - 21O_6^4) + B_6^t(O_6^2 - O_6^6), \quad (1)$$

where the last term is absent in the ordinary cubic symmetry O_h. Its presence does not affect the degeneracy of each sublevel when compared with that of the O_h group, but some eigenfunctions and eigenvalues may be appreciably different.[8] The knowledge of the CF levels, especially the ground state, is essential to understand the role of the $4f$ electrons in these compounds. However, in spite of the large amount of work invested, the CF ground state is still unclear in several of these systems.[11,12]

Electron spin resonance (ESR) has been used for more than half a century to examine a wide variety of compounds.[10] It is a very useful and highly sensitive technique for studying spin correlations. It provides information about CF effects, site symmetry, valence of the paramagnetic ions, g value, fine and hyperfine parameters, etc. Moreover, the sample size required for ESR is typically less than ~ 4 mm^3, i.e., much smaller than that needed for most other techniques. When the compound is not paramagnetic, ESR can still provide useful information by doping the matrix with a small amount of paramagnetic ions such as Nd^{3+}, Gd^{3+}, Dy^{3+}, Er^{3+}, and Yb^{3+}. The ESR spectra of the impurities allow one not only to learn about the impurity, but also to study the properties of the host lattice. In cases where the first excited state is separated from the ground state by an energy of the order of the temperature at which the data is taken, a field-induced change in the g value[13] and an exponentially activated T dependence of the linewidth[14,15] may be expected. Moreover, the ESR of an excited state could also be observed.[16] Thus, by measuring the ESR at different frequencies and temperatures of various R impurities, one may obtain an accurate determination of their ground state and, in some cases, the full set of CFPs determining the overall splitting of the ground J multiplet.

Mesquita *et al.*[17] and Martins *et al.*[18] measured the ESR spectra of $Ce_{1-x}R_xFe_4P_{12}$ (R=Nd, Dy, Er, Yb; $x \lesssim 0.005$) up to 4.2 K. Our data, taken in the same range of T, agree with those published previously. The data in Refs. 17 and 18 were analyzed assuming H_{CF} for the cubic group, i.e., Eq. (1) without the B_6^t term. In particular, the unexpected g value of 6.408(3) measured for the Kramers doublet ground state of Er^{3+} in $CeFe_4P_{12}$ cannot be explained if the term $B_6^t(O_6^2 - O_6^6)$ is not included in H_{CF}. By using the H_{CF} given in Eq. (1) and measuring up to $T \cong 50$ K to populate the excited states, the ESR data for the various R impurities can be explained and the full set of CFPs is determined.

The last term in Eq. (1) is usually of secondary importance. ESR is the second technique known to us where this

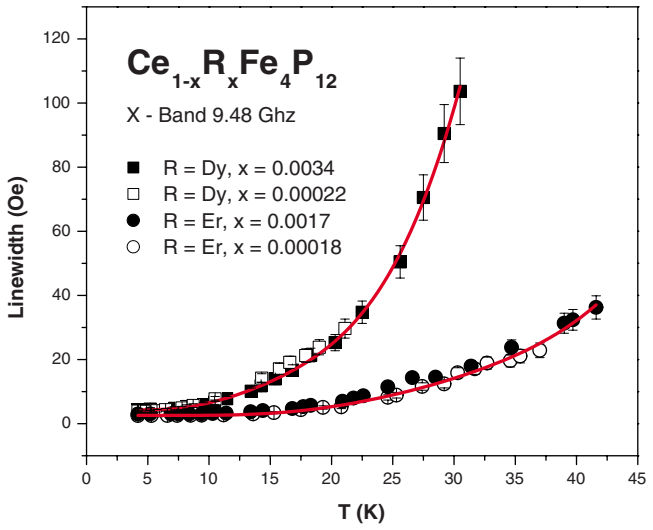

FIG. 1. (Color online) T dependence of ΔH of X-band ESR for Dy^{3+} and Er^{3+} in $Ce_{1-x}R_xFe_4P_{12}$ (R=Dy, Er). The solid lines are fits to Eq. (6) leading to the following parameters for Dy: a =4.0(4) Oe, Δ_1=40(8) K, Δ_2=135(30) K, c_1=0.0015(2) Oe/K^3, and c_2=0.0020(2) Oe/K^3; and for Er: a=3.3(3) Oe, Δ_1 =85(15) K, Δ_2=300(100) K, c_1=0.0003(1) Oe/K^3, and c_2 =0.0002(1) Oe/K^3.

term cannot be ignored. The other examples are the crystalline field potential of $PrOs_4Sb_{12}$ and $PrFe_4Sb_{12}$ measured by inelastic neutron scattering.[12,19,20] In those compounds the B_6^t term rules out the non-Kramers doublet Γ_3 as the ground state, in favor of the Γ_1 singlet.

II. EXPERIMENTAL

Single crystals of $Ce_{1-x}R_xFe_4P_{12}$ (R=Nd, Dy, Er, Yb; $x \lesssim 0.003$) were grown in a molten Sn flux according to the method described in Ref. 21. Within the accuracy of microprobe analysis the crystals studied are found to be uniform. The R concentrations were determined from the H and T dependence of the magnetization, $M(H,T)$. $M(H,T)$ measurements were taken in a Quantum Design magnetic property measurement system (MPMS) superconducting quantum interference device (SQUID) dc magnetometer. The crystals used were about $2\times2\times2$ mm^3 with perfect natural crystallographic grown faces. The cubic structure (space group $Im3$) and phase purity were checked by x-ray powder diffraction. The ESR spectra were taken in Bruker X- (9.48 GHz) and Q-band (34.4 GHz) spectrometers using appropriated resonators coupled to a T controller of a helium gas flux system for 4.2 K$\lesssim T \lesssim$300 K. The R^{3+} resonances show Dysonian (metallic) line shape ($A/B \approx 2.5$) corresponding to a microwave skin depth [$\delta = 1/(\pi\mu_0\sigma\nu)^{1/2}$] smaller than the size of the crystals.[22] The low-T metallic character of the compound is associated to the thermally activated conductivity [$\simeq 10^{-3}(\Omega\ \mathrm{cm})^{-1}$] reported for this material at low T.[21]

III. RESULTS

Figure 1 shows the T dependence of the X-band ESR linewidth, ΔH, for the Kramers doublet ground state of Dy^{3+} and Er^{3+} in $CeFe_4P_{12}$. Within the experimental accuracy, the linear T term is negligible at low T, in agreement with previous measurements.[17] This indicates that there is no spin-lattice relaxation via an exchange interaction with the conduction electrons (ce) (Korringa relaxation).[23,24] Q-band data (not shown here) are similar to the data presented in Fig. 1 with slightly larger ($\lesssim$15%) residual linewidth, $\Delta H(T=0\ \mathrm{K})$; i.e., no inhomogeneous broadening is observed. Thus, the exponential increase in ΔH at high T results from a homogeneous line broadening due to a phonon spin-lattice relaxation process involving the excited CF levels (see below).[14,15] For Yb^{3+} in $CeFe_4P_{12}$ a T-independent (not shown) resonance of ΔH=8(2) Oe corresponding to a Kramers doublet ground state was observed up to $T \simeq 40$ K. Figure 2 displays $M(H,T)$ for the same samples.

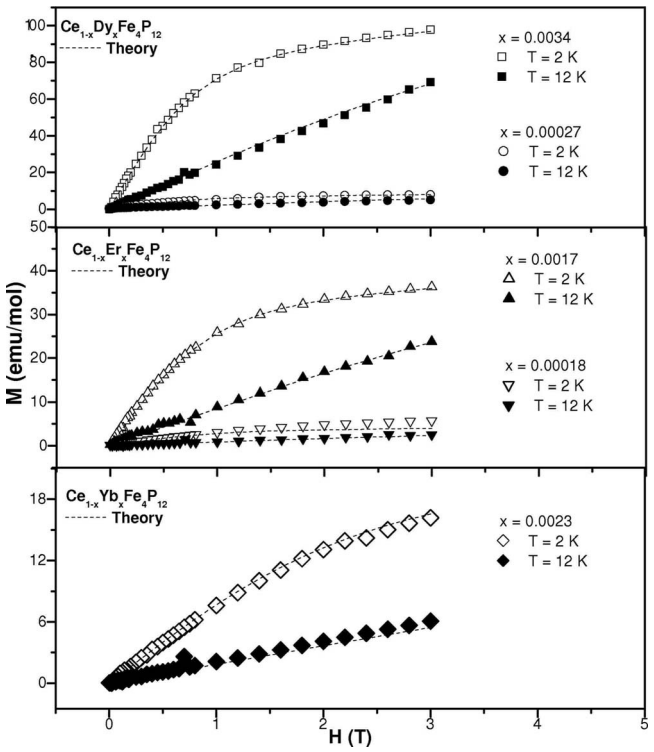

FIG. 2. $M(H,T)$ for Dy^{3+}, Er^{3+}, and Yb^{3+} in $Ce_{1-x}R_xFe_4P_{12}$ (R=Dy, Er, Yb). The dashed curves are the calculated $M(H,T)$ from Eq. (8) using the CFPs from Table I. The contribution of the sample holder and host lattice to the measured magnetization has been subtracted.

For Nd^{3+} in $CeFe_4P_{12}$ the ground state corresponds to an anisotropic quadruplet. The g-value anisotropy has been obtained by measuring the two allowed transitions within this quadruplet for the field on the (110) plane at T=4.2 K.[18]

The resonances associated to the above ESR data correspond to the R^{3+} I=0 isotopes. We have also observed the resonances corresponding to various R^{3+} isotopes with $I \neq 0$, which, at low T, show the same features already reported.[17,18] Furthermore, the T dependence of the ESR intensity for the observed resonances follows approximately a Curie-Weiss law at low T. This indicates that the resonances arise from the ground state of the CF split J multiplet. The measured g values and degeneracy of the ground states are displayed in Table I.

TABLE I. ESR and CFPs for $Ce_{1-x}R_xFe_4P_{12}$ (R=Nd, Dy, Er, Yb). Ground-state degeneracy is abbreviated "gsd" and "Anis" denotes anisotropic ground state. The symbol (*) denotes a result obtained from Dy^{3+} data.

R^{3+}	gsd	g_{expt}	g_{calc}	x	y	W (K)	B_4^c (mK)	B_6^c (mK)	B_6^t (mK)
Nd^{3+}	4	Anis	Anis	−0.566	0.00	<0	>0	<0	0.00
Dy^{3+}	2	7.438(7)	7.43(3)	0.32	0.40	0.92(16)	2.9(6)	0.027(6)	0.28(6)
Er^{3+}	2	6.408(3)	6.40(6)	−0.16	0.45	1.6(3)	−2.3(5)	0.053(10)	0.54(10)
Yb^{3+}	2	2.575(2)	2.6(1)	0.54	0.08	7(2)*	58(17)	2.3(7)	24(7)

IV. ANALYSIS AND DISCUSSION

We now add the Zeeman term $g_J\mu_B\mathbf{H}\cdot\mathbf{J}$ to Eq. (1), where g_J is the Landé g factor, μ_B is the Bohr magneton, $\mathbf{J}$ is the total angular momentum for each R ion, and $\mathbf{H}$ is the dc magnetic field. Following Lea, Leask, and Wolf[25] (LLW), the Hamiltonian can be parametrized as

$$H_{CFZ} = W\left\{(1-|y|)\left[x\frac{O_4^c}{F_4^0} + (1-|x|)\frac{O_6^c}{F_6^0}\right] + y\frac{O_6^t}{F_6^2}\right\} + g_J\mu_B\mathbf{H}\cdot\mathbf{J}, \quad (2)$$

where we denoted $O_4^0+5O_4^4$ by O_4^c and similarly the sixth-order terms by O_6^c and O_6^t. The coefficients of Eq. (1) are rewritten as $B_4^c=(1-|y|)xW/F_4^0$, $B_6^c=(1-|y|)(1-|x|)W/F_6^0$, and $B_6^t=yW/F_6^2$. The coefficients F_n^m are tabulated in Ref. 26 for various values of J. The above is a generalization of the LLW Hamiltonian that includes the O_6^t term.[8,25] Our parametrization is slightly different from that in Ref. 8 and has the advantage that the entire range of the CFPs is accounted for within the finite intervals $(-1\le x\le 1)$ and $(-1\le y\le 1)$.

By diagonalizing H_{CFZ} we obtained the CF wave functions and energies for each of the R in units of W as a function of x and y. Then, for a small H the doublet ground state (Γ_i, i=5, 6, or 7) the g value can be calculated ($g=2g_J|\langle\Gamma_i|S_z|\Gamma_i\rangle|$). For finite field and at resonance, g can be obtained from the Zeeman splitting of the doublet, $\Delta E(H)=h\nu=g\mu_BH$. Figure 3 shows the x and y dependence of the g value for the ground state of Er^{3+} (J=15/2, g_J=6/5, and $W>0$) in a color scale. For y=0 and variable x, we obtain the expected g values of 6.000 (orange) for the Γ_6 and 6.800 (yellow) for the Γ_7 doublets.[25] The white region in Fig. 3 corresponds to the quadruplet ground states. Thus, a g value of 6.408 corresponds neither to a Γ_6 nor to a Γ_7 (y=0). For $y\neq 0$ the g value decreases to and approaches zero for large values of y (black region). Hence, the measured g value of ~6.4 for Er^{3+} corresponds to a doublet ground state with $y\neq 0$. Such a g value is obtained for the set of (x,y) values indicated by the dashed blue line in Fig. 3. The results shown in Fig. 3 do not depend on the sign of y.

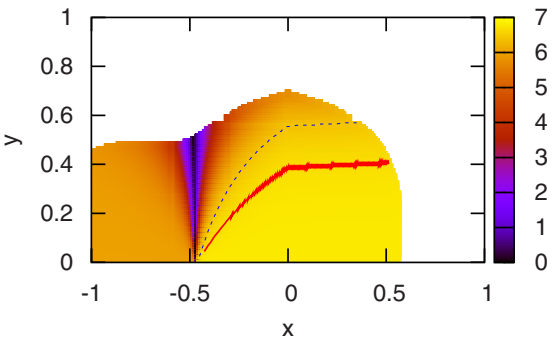

FIG. 3. (Color online) The color scale shows the ground-state theoretical g values for Er^{3+} (J=15/2, g_J=6/5, and $W>0$) as a function of (x,y). The blue dashed line indicates the set of (x,y) values corresponding to the experimental g=6.40. The red line corresponds to the (x,y) values for Dy^{3+} (J=15/2, g_J=4/3, and $W>0$) and measured g=7.438 (the experimental uncertainty of the g value is about the width of those lines).

The same procedure was followed with the measured g values for Dy^{3+} (J=15/2 and g_J=4/3) and Yb^{3+} (J=7/2 and g_J=8/7) impurities. To be able to present the g values of Dy^{3+} in Fig. 3, we rescaled them by the g_J ratio between Dy^{3+} and Er^{3+} ($g_J^{Dy}/g_J^{Er}=10/9$). The (x,y) values corresponding to the experimental g value for Dy^{3+} are given by the red curve in Fig. 3. The results for Yb^{3+} are similar but are not shown in Fig. 3.

The B_n^m parameters are angular momentum effective values of the *actual* CFP A_n^m defined in real space. The B_n^m and A_n^m are related by $B_n^m=\langle r^n\rangle\theta_nA_n^m$.[26] Here θ_n is a geometrical factor arising from the addition of angular momenta. The substitution of a weakly intermediate valence Ce ion by an R^{3+} impurity may distort the electron density in the neighborhood of the defect. However, the host perturbation by the R^{3+} impurities should be comparable for Er^{3+}, Dy^{3+}, and Yb^{3+} ions. Therefore, the *actual* CFPs A_n^m should not depend much on the ion R. Thus, if R_1 and R_2 denote two rare-earth impurities, it is possible to relate their CFPs,[26]

$$\frac{B_n^m(R_1)}{\langle r^n(R_1)\rangle\theta_n(R_1)} = \frac{B_n^m(R_2)}{\langle r^n(R_2)\rangle\theta_n(R_2)}. \quad (3)$$

Defining

$$\beta = \frac{\langle r^4(R_2)\rangle}{\langle r^6(R_2)\rangle}\frac{\langle r^6(R_1)\rangle}{\langle r^4(R_1)\rangle},$$

$$\delta = \frac{\langle r^6(R_1)\rangle}{\langle r^6(R_2)\rangle},$$

$$\xi = \frac{\theta_4(R_2)}{\theta_4(R_1)}\frac{\theta_6(R_1)}{\theta_6(R_2)}\frac{F_6^0(R_1)}{F_6^0(R_2)}\frac{F_4^0(R_2)}{F_4^0(R_1)},$$

$$\gamma = \frac{F_6^0(R_1)}{F_6^0(R_2)} \frac{F_6^2(R_2)}{F_6^2(R_1)},$$

$$\eta = \frac{F_6^2(R_1)}{F_6^2(R_2)} \frac{\theta_6(R_1)}{\theta_6(R_2)},$$

we obtain the following relations among the sets of parameters (x_2, y_2, W_2) and (x_1, y_1, W_1) for the two ions:

$$x_2 = \frac{\xi\beta}{1-(1-|\xi\beta|)|x_1|} x_1,$$

$$y_2 = \left[1 + \frac{(1-|x_1|)(1-y_1)}{\gamma y_1 \left(1 - \left| \frac{\xi\beta x_1}{1-(1-|\xi\beta|)|x_1|} \right| \right)} \right]^{-1}, \quad (4)$$

and

$$W_2 = \eta\delta W_1 \left[y_1 + \frac{(1-|x_1|)(1-y_1)}{\gamma \left(1 - \left| \frac{\xi\beta x_1}{1-(1-|\xi\beta|)|x_1|} \right| \right)} \right]^{-1}, \quad (5)$$

where ξ, γ, and η are *geometrical* parameters that only depend on θ_n and F_n^m (their values are tabulated in Ref. 26). On the other hand, β and δ depend on the expectation values $\langle r^n(R)\rangle$. β enters the expression for x_2 and y_2, while in order to obtain W_2 also δ is needed. The values for $\langle r^n(R)\rangle$ were computed in Ref. 27 for the free (unperturbed) rare-earth ions. In general, the $\langle r^n(R)\rangle$ values depend on the host, in particular whether it is an insulating[28] or a metallic[29] environment. Their values may be obtained from *ab initio* calculations, which are beyond the scope of this work. Nonetheless, β and δ depend on the $\langle r^n(R_1)\rangle/\langle r^n(R_2)\rangle$ ratios that, for Dy^{3+}, Er^{3+}, and Yb^{3+}, in a given lattice (whether insulator[27,28] or metals[29]) present differences smaller than 5%. In other words, the changes in $\langle r^n(R)\rangle$ from the free-ion values are about the same for the various R when located in the same environment. As $CeFe_4P_{12}$ is a small-gap semiconductor, for β and δ we shall assume values close to those for an insulator. Here we assume that the values are within $\pm 10\%$ of the insulating ones.[28]

The blue curve in Fig. 4 again shows the (x,y) parameters for Er^{3+} (see Fig. 3). Using Eq. (4), the set of (x,y) values for Dy^{3+} and Yb^{3+} that satisfy the measured ground-state g values may be transformed to the (x,y) space corresponding to Er^{3+}. The results for Yb^{3+} and Dy^{3+} are shown in Fig. 4 by the red and black lines, respectively. The width of these lines includes the uncertainty of β and experimental error bars of the measured g values. Notice that the lines for Dy^{3+}, Er^{3+}, and Yb^{3+} all intersect at a single point $[x \approx -0.16(3), y \approx 0.45(3)]$. The three ions have the same charge and a similar size; therefore, we may assume that the *actual* CFPs are about the same for these impurities in $CeFe_4P_{12}$. This suggests that the ratios involving the *actual* CFPs are $A_4^c\langle r^4(R)\rangle/A_6^c\langle r^6(R)\rangle \approx -2.0$ and $A_6^t/A_6^c \approx 10$ for the three impurities. Now these Er^{3+} (x,y) values are transformed back to obtain the (x,y) values for Dy^{3+} and Yb^{3+}, which are listed in Table I. Notice that the (x,y) values for Dy^{3+} and Yb^{3+} are obtained by using their experimental g values and the assumption of similar crystal fields.

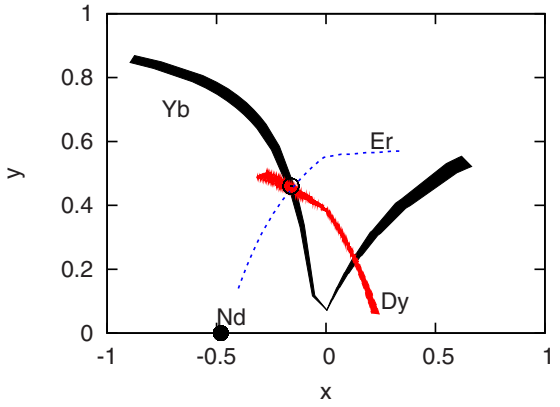

FIG. 4. (Color online) Set of (x,y) values satisfying the ground-state g values of the studied R^{3+} ions, transformed into the Er^{3+} (x,y) space by Eq. (4). The open circle indicates the point where Dy^{3+}, Er^{3+}, and Yb^{3+} share the same ratios, $A_4^c\langle r^4(R)\rangle/A_6^c\langle r^6(R)\rangle \approx -2.0$ and $A_6^t/A_6^c \approx 10$ (see text).

The above is valid independently of the energy scaling parameter W. The values of W for all three impurities can be determined if the W for one of them is known [see Eq. (5)]. W can be estimated from the T dependence of ΔH data. The solid lines seen in Fig. 1 are the best fit of the measured ΔH for Dy^{3+} and Er^{3+} in $CeFe_4P_{12}$ to the expression

$$\Delta H = a + c_1 \frac{\Delta_1^3}{[e^{\Delta_1/kT} - 1]} + c_2 \frac{\Delta_2^3}{[e^{\Delta_2/kT} - 1]}, \quad (6)$$

where a is the residual linewidth. The relaxation is through phonon modes and requires the coupling of phonons between the ground and excited CF states. We consider here the two lowest excited CF states with nonvanishing matrix elements from the ground state and denote the excitation energies with $\Delta_{1,2}$. The coefficients $c_{1,2}$ are given by $(3k_B^2/2\pi h^4 \rho v^5) M_{1,2}^2$ (ρ is the host density, v is the sound velocity, and $M_{1,2}^2$ is the sum of the square of the matrix elements of the dynamic crystal field potential).[14,15] The parameter values resulting from the fits are given in the caption of Fig. 1.

By using the values of (x,y), Δ_1, and Δ_2 (see Fig. 1), we obtain $W_{Dy} = 0.92(16)$ K and $W_{Er} = 1.6(3)$ K. The resulting energy levels for Dy^{3+} and Er^{3+} ions are shown in Fig. 5. On the other hand, using W_{Dy} and Eq. (5) we can obtain W for the other ions. In particular, for Er^{3+} we obtain $W_{Er}^* = 1.3(4)$ K, where the error bar includes 20% of experimental errors and 10% from the uncertainty of δ. We see that, within the error bars, the values W_{Er} and W_{Er}^* agree. Using again W_{Dy} we determined $W_{Yb}^* = 7(2)$ K. The Yb^{3+} energy levels are also shown in Fig. 5. Once the set of (x,y) and W parameters is known for a given R, their corresponding CFPs B_n^m are calculated (see Table I).

Assuming that the $\langle r^n(R)\rangle$ values are within 10% of their values in insulators,[28] the *actual* CFPs A_n^m can be estimated,

$$A_4^c \cong -33(10) \text{ K}/a_0^4,$$

$$A_6^c \cong 4(1) \text{ K}/a_0^6,$$

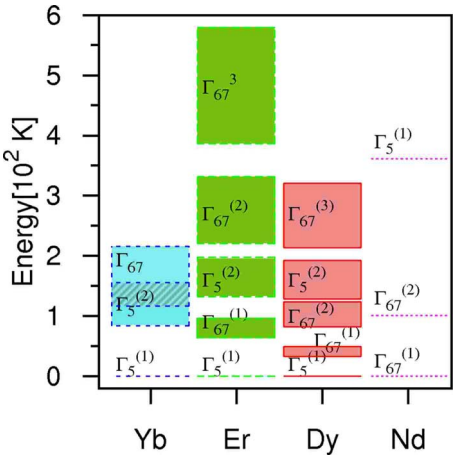

FIG. 5. (Color online) CF energy levels for the studied R^{3+} ions in $CeFe_4P_{12}$. For Nd^{3+} we used arbitrarily $W_{Nd}=-5$ K. Thus, if the actual W_{Nd} value is known the Nd^{3+} energy levels should be scaled by $-W_{Nd}/5$ K. The heights of the dotted line boxes indicate the uncertainty of the energy levels.

$$A_6^t \cong 44(15)\ \text{K}/a_0^6, \tag{7}$$

where a_0 is the Bohr radius. The main sources of error are the experimental Δ_1 and theoretical δ uncertainties.

For Nd^{3+} the (x,y) values that account for the measured anisotropic g values of the quadruplet ground state are given in Table I. These values correspond to a point in the Er^{3+} (x,y) space (filled circle in Fig. 4), which is different than that for the other R^{3+} ions. This suggests that the large Nd^{3+} ionic radius, as compared with those of the other R^{3+} and the intermediate valence of the Ce ions, probably causes a large local crystal distortion close to the Nd^{3+} site. Additional experimental information, involving the excited CF levels, would be needed to determine W_{Nd} in this compound. Therefore, the complete set of *actual* CFPs A_n^m for Nd^{3+} cannot be given. Nevertheless, the (x,y) values for Nd^{3+} are compatible with $W_{Nd}<0$. In Fig. 5 we present the Nd^{3+} energy levels using arbitrarily $W_{Nd}=-5$ K (see caption of Fig. 5).

The CF splittings of the J multiplet determine $M(H,T)$,

$$M(H,T) = \frac{\sum_{i=1}^{2J+1} m_i(H) e^{-E_i(H)/k_B T}}{\sum_{i=1}^{2J+1} e^{-E_i(H)/k_B T}}, \tag{8}$$

where $m_i(H)$ and $E_i(H)$ are the magnetization and energy eigenvalue of each eigenstate of the Hamiltonian [Eq. (2)] computed at a *finite* H using Eq. (8) and the CFPs B_n^m given in Table I. The dashed curves in Fig. 2 show the calculated magnetization, $M(H,2\ \text{K})$ and $M(H,12\ \text{K})$, for two concentrations of Dy^{3+}, Er^{3+}, and Yb^{3+} as compared to the experimental data. In all cases the sample holder diamagnetism was previously determined and subtracted from the total magnetization. Also, the paramagnetic contribution of the undoped $CeFe_4P_{12}$ host lattice was measured and subtracted. At low T ($2\ \text{K} \leq T \leq 12\ \text{K}$) that magnetization is less than 10% of the samples doped with Er ($x=0.0017$) and Dy ($x=0.0034$) and ~30% of the one doped with Yb ($x=0.0023$).

V. CONCLUSIONS

The filled skutterudite $CeFe_4P_{12}$ compound is a small-gap ($\simeq 1500$ K) semiconductor.[21] Hence, the R^{3+} spin-lattice relaxation via an exchange interaction with ce is inhibited (Korringa process),[23,24] since the ce must be promoted via exponential activation. This is verified by the absence of a linear T term in our low-T ΔH data (see Fig. 1). Similarly, a g shift (Knight shift)[24] is not expected. Therefore, the shift of the g value of the Kramers ground doublet relative to that in O_h symmetry ($y=0$) is due to the $B_6^t(O_6^2-O_6^6)$ term in H_{CF}. For O_h symmetry the Kramers doublet g values are unique (independent of the CFPs)[25] and the exchange coupling in a metallic host is simply obtained from the g shift of the resonance. Our calculation showed that the presence of the additional term results always in an isotropic g value and a negative g shift for the doublet ground states for $J=7/2$ and 15/2. For impurities in metallic hosts with T_h symmetry, when studied by ESR, a negative g shift results in a complication to evaluate the sign and magnitude of the exchange interaction between the R^{3+} localized magnetic moment and the ce.

In summary, in this work we measured the ESR for Dy^{3+}, Er^{3+}, and Yb^{3+} ions doped into the filled skutterudite $CeFe_4P_{12}$ with T_h structure. We obtained the three CFPs B_n^m, determined the CF ground state, explained the unexpected Er^{3+} g value, and found the CF overall splitting for the J ground-state multiplet. With the obtained CFPs we could fit the low-T $M(H,T)$ of the crystals used in the ESR experiments. Moreover, our working assumption that the *actual* CFPs A_n^m are about the same for Dy^{3+}, Er^{3+}, and Yb^{3+} in this compound turned out to be very plausible. A similar work could be carried out on undoped compounds such as $LnFe_4P_{12}$, for Ln=Nd, Gd, Dy, etc., all Kramers ions with magnetic ground multiplet. Moreover, this work and our preliminary ESR data in the doped unfilled skutterudites $CoSb_3$ put in evidence the importance of the extra $B_6^t(O_6^2-O_6^6)$ term in H_{CF} for compounds with T_h symmetry. In addition, we emphasized the extra caution we need to have when ESR is used to determine the exchange parameter in metallic compounds with T and T_h symmetry.

ACKNOWLEDGMENTS

The work at UNICAMP was supported by FAPESP and CNPq, Brazil. P.S. was supported by the U.S. Department of Energy via Grant No. DE-FG02-98ER45707.

[1] E. Bauer, A. Grytsiv, Xing-Qiu Chen, N. Melnychenko-Koblyuk, G. Hilscher, H. Kaldarar, H. Michor, E. Royanian, G. Giester, M. Rotter, R. Podloucky, and P. Rogl, Phys. Rev. Lett. **99**, 217001 (2007).
[2] W. Jeitschko and D. Braun, Acta Crystallogr., Sect. B: Struct. Crystallogr. Cryst. Chem. **33**, 3401 (1977).
[3] E. D. Bauer, A. Slebarski, E. J. Freeman, C. Sirvent, and M. B. Maple, J. Phys.: Condens. Matter **13**, 4495 (2001).
[4] N. R. Dilley, E. J. Freeman, E. D. Bauer, and M. B. Maple, Phys. Rev. B **58**, 6287 (1998).
[5] N. Takeda and M. Ishikawa, J. Phys.: Condens. Matter **13**, 5971 (2001).
[6] B. C. Sales, D. Mandrus, and R. K. Williams, Science **272**, 1325 (1996).
[7] C. Sekine, K. Akita, N. Yanase, I. Shirotani, I. Inagawa, and C. Lee, Jpn. J. Appl. Phys., Part 1 **40**, 3326 (2001).
[8] K. Takegahara, H. Harima, and A. Yanase, J. Phys. Soc. Jpn. **70**, 1190 (2001).
[9] T. Inui, Y. Tanabe, and Y. Onodera, *Group Theory and Its Applications in Physics* (Springer, Berlin, 1966).
[10] A. Abragam and B. Bleaney, *EPR of Transition Ions* (Clarendon, Oxford, 1970).
[11] Y. Nakanishi, T. Kumagai, M. Oikawa, T. Tanizawa, M. Yoshizawa, H. Sugawara, and H. Sato, Phys. Rev. B **75**, 134411 (2007); T. Yanagisawa, W. M. Yuhasz, P.-C. Ho, M. Brian Maple, H. Watanabe, T. Ueno, Y. Nemoto, and T. Goto, J. Magn. Magn. Mater. **310**, 223 (2007); W. M. Yuhasz, N. A. Frederick, P.-C. Ho, N. P. Butch, B. J. Taylor, T. A. Sayles, M. B. Maple, J. B. Betts, A. H. Lacerda, P. Rogl, and G. Giester, Phys. Rev. B **71**, 104402 (2005); C. R. Rotundu, K. Ingersent, and B. Andraka, *ibid.* **75**, 104504 (2007); W. M. Yuhasz, P.-C. Ho, T. A. Sayles, T. Yanagisawa, N. A. Frederick, M. B. Maple, P. Rogl, and G. Giester, J. Phys.: Condens. Matter **19**, 076212 (2007); C. P. Yang, H. Wang, and K. Iwasa, Appl. Phys. Lett. **89**, 082508 (2006).
[12] E. A. Goremychkin, R. Osborn, E. D. Bauer, M. B. Maple, N. A. Frederick, W. M. Yuhasz, F. M. Woodward, and J. W. Lynn, Phys. Rev. Lett. **93**, 157003 (2004).
[13] S. Oseroff, M. Passeggi, D. Wohlleben, and S. Schultz, Phys. Rev. B **15**, 1283 (1977).
[14] D. Davidov, C. Rettori, A. Dixon, K. Baberschke, E. P. Chock, and R. Orbach, Phys. Rev. B **8**, 3563 (1973).
[15] G. E. Barberis, D. Davidov, J. P. Donoso, C. Rettori, J. F. Suassuna, and H. D. Dokter, Phys. Rev. B **19**, 5495 (1979).
[16] C. Rettori, E. Weber, J. P. Donoso, F. C. G. Gandra, and, G. E. Barberis, Solid State Commun. **39**, 1025 (1981).
[17] R. N. de Mesquita, G. E. Barberis, C. Rettori, M. S. Torikachvili, and M. B. Maple, Solid State Commun. **74**, 1047 (1990).
[18] G. B. Martins, M. A. Pires, G. E. Barberis, C. Rettori, and M. S. Torikachvili, Phys. Rev. B **50**, 14822 (1994).
[19] K. Kuwahara, K. Iwasa, M. Kohgi, K. Kaneko, S. Araki, N. Metoki, H. Sugawara, Y. Apki, and H. Sato, J. Phys. Soc. Jpn. **73**, 1438 (2004).
[20] E. Bauer, A. Grytsiv, P. Rogl, W. Kockelmann, A. D. Hillier, E. A. Goremychkin, D. T. Adroja, and J.-G. Park, J. Magn. Magn. Mater. **310**, 286 (2007).
[21] G. P. Meisner, M. S. Torikachvili, K. N. Yang, M. B. Maple, and R. P. Guertin, J. Appl. Phys. **57**, 3073 (1985).
[22] G. Feher and A. F. Kip, Phys. Rev. **98**, 337 (1955); F. J. Dyson, *ibid.* **98**, 349 (1955); G. E. Pake and E. M. Purcell, *ibid.* **74**, 1184 (1948).
[23] J. Korringa, Physica (Amsterdam) **16**, 601 (1950); H. Hasegawa, Prog. Theor. Phys. **21**, 1093 (1959).
[24] C. Rettori, D. Davidov, R. Orbach, E. P. Chock, and B. Ricks, Phys. Rev. B **7**, 1 (1973).
[25] K. R. Lea, M. J. M. Leask, and W. P. Wolf, J. Phys. Chem. Solids **23**, 1381 (1962).
[26] M. T. Hutchings, Solid State Phys. **16**, 227 (1964).
[27] R. E. Freeman and A. J. Watson, Phys. Rev. **127**, 2058 (1962).
[28] A. J. Freeman and J. P. Desclaux, J. Magn. Magn. Mater. **12**, 11 (1979).
[29] L. Steinbeck, M. Richter, H. Eschrig, and U. Nitzsche, Phys. Rev. B **49**, 16289 (1994).